IEEE Access
Multidisciplinary ⋮ Rapid Review ⋮ Open Access Journal

Received March 18, 2020, accepted April 2, 2020, date of publication April 6, 2020, date of current version April 22, 2020.

Digital Object Identifier 10.1109/ACCESS.2020.2986075

Bandwidth, Power and Trajectory Optimization for UAV Base Station Networks With Backhaul and User QoS Constraints

YINGQIAN HUANG[1], MIAO CUI[1], GUANGCHI ZHANG[1], AND WEI CHEN[2]
[1]School of Information Engineering, Guangdong University of Technology, Guangzhou 510006, China
[2]Institute of Environmental Geology Exploration of Guangdong Province, Guangzhou 510080, China

Corresponding author: Miao Cui (cuimiao@gdut.edu.cn)

This work was supported in part by the National Natural Science Foundation of China under Grant 61571138, in part by the Science and Technology Plan Project of Guangdong Province under Grant 2017B090909006 Grant 2018A050506015, Grant 2019B010119001, and Grant 2020A050515010, in part by the Special Support Plan for High-Level Talents of Guangdong Province under Grant 2019TQ05X409, and in part by the Science and Technology Plan Project of Guangzhou City under Grant 201904010371.

ABSTRACT This paper considers an unmanned aerial vehicle (UAV) base station (BS) network with delay-sensitive users and delay-tolerant users on the ground, which have different quality-of-service (QoS) requirements. In the network, the backhaul link connecting the backhaul gateway and the UAV-BS shares the same spectrum with the data links connecting the UAV-BS and the users due to spectrum scarcity. To improve the rate performance of the delay-tolerant users and to guarantee the QoS of the delay-sensitive users, we aim to maximize the minimum rate of the delay-tolerant users by jointly optimizing the bandwidths of the backhaul link and the data links, the transmit power allocated to different users and the trajectory of the UAV-BS, subject to the constraints on UAV mobility, total bandwidth, total transmit power, backhaul data rate, and minimum rate requirements of the delay-sensitive users. Although the formulated problem is non-convex and difficult to solve optimally, we propose an efficient algorithm to find a suboptimal solution to it. Simulation results show that the proposed joint optimization algorithm achieves significantly higher minimum user rate than the benchmark schemes.

INDEX TERMS UAV base station, bandwidth and power allocation, trajectory optimization, backhaul constraint, quality-of-service.

I. INTRODUCTION

After decades of rapid development, unmanned aerial vehicles (UAVs) have been widely used in military, transportation, agriculture, logistics, and many other fields, and have brought a lot of changes to people's lives, due to their advantages such as high maneuverability, easy deployment, and low cost. With the rising of the fifth-generation (5G) wireless communication era, UAVs have found their roles in assisting wireless communication, which help to boost the performance of 5G networks and satisfying the quality-of-service (QoS) requirements of users [1]. The communication assisted by UAVs is called UAV-enabled communication, where UAVs can be used as aerial base stations (BSs) [2], [3] or relays [4], [5], and is especially suitable in emergent cases like data traffic congestions or natural disasters. As compared to terrestrial communications, one key advantage of UAV-enabled communications is that the channels between UAVs and ground nodes usually have high quality, since they are dominated by line-of-sight (LoS) links with high probability [6]–[8]. Furthermore, the communication performance of UAV-enabled communications can be improved by exploiting UAVs' high mobility via appropriate trajectory design [2]–[5]. Although such performance improvement can also be achieved in the unmanned ground vehicle (UGV) communications [9], [10], designing UAVs' trajectories has much fewer constraints than designing UGVs' routes, such as obstructions and road restrictions, thus UAV-enabled communications have more degree of freedom in performance optimization.

After years of investigation, UAV-enabled communication still faces some key technological difficulties that have not been tackled, and the potential advantages of UAVs have not been fully exploited. For example, Refs. [11] and [12] consider employing UAVs as quasi-stationary UAV base stations (UAV-BSs), and Ref. [13] proposes an energy-saving

The associate editor coordinating the review of this manuscript and approving it for publication was Cunhua Pan.

scheme for quasi-stationary UAV relays. However, in these works, the trajectories of the UAVs have not been optimized to fully use the high maneuverability advantage of the UAVs to improve communication performance. In fact, in a UAV-enabled communication network, jointly optimizing the communication resource and the UAV trajectories according to the network's dynamics can significantly boost the communication performance and is a promising research direction.

Motivated by this, several research works have been conducted on the joint trajectory optimization and resource allocation schemes in UAV-enabled communication networks. In [2] and [3], wireless networks with a single UAV-BS and multiple UAV-BSs have been considered, respectively, where user association and trajectories of the UAV-BSs have been jointly optimized to maximize the minimum rate of all users. In [14]–[16], joint power allocation and trajectory optimization of UAV-BSs have been investigated for secure communication under different system setups. Refs. [4] and [5] study joint resource allocation and trajectory optimization in UAV relay systems. The above works consider fixed bandwidth in each data link, whose performance can be further improved by adjusting the bandwidth of each data link according to the channel and system dynamics adaptively. In [17], joint optimization on deployment location, bandwidth, and beamwidth of a UAV-BS have been investigated. In [18], joint optimization on deployment location, power, and bandwidth of a UAV-BS coexisting with a device-to-device communication network has been investigated. In [19], joint bandwidth, power and trajectory optimization for a multi-hop UAV relay system has been investigated, where the end-to-end throughput has been maximized.

The aforementioned works mainly focus on optimizing the bandwidths of the data links that connect the UAV-BS and the users but ignores the backhaul link that connects the UAV-BS and the core network [20]. In practice, when the bandwidth of a backhaul link is limited, the backhaul link may limit the overall performance of a UAV-BS network, so communication optimization in the network should take the backhaul link constraint into account. In [21], the throughput of a UAV-BS's backhaul that is formed by multi-hop UAV relays has been optimized. In [22], joint optimization on deployment and user association of a static multi-UAV-BS network with backhaul constraint has been investigated. Besides the backhaul issue, satisfying the QoS requirements of the users is important to a UAV-BS network. In [23], power consumption is minimized subject to the user QoS constraints. In [24], the deployment of a static UAV-BS has been optimized to satisfying the user QoS requirement. To the best of our knowledge, communication optimization of a mobile UAV-BS with both the backhaul constraint and different user QoS requirements has not been addressed by existing works.

In this paper, we consider improving the communication performance of a UAV-BS network with the backhaul constraint, where the users are divided into two groups based on their different QoS requirements, i.e., delay-tolerant users and delay-sensitive users, as shown in Fig. 1. Due to spectrum scarcity, the backhaul link that connects the backhaul gateway and the UAV-BS shares the same spectrum with the data links that connect the UAV-BS and the users. Subject to the backhaul constraint that restricts the sum of data rates of all users not exceeding the rate of backhaul and the minimum rate requirements of the delay-sensitive users, we jointly optimize the bandwidths of the backhaul link and the data links, the transmit power allocated to different users and the trajectory of the UAV-BS to maximize the minimum rate of the delay-tolerant users. Although the formulated problem is difficult to solve due to its non-convex structure and coupling of optimization variables, we propose an efficient algorithm to find a suboptimal solution to it, based on the alternating optimization and successive convex approximation techniques. Simulation results show the fundamental minimum user rate limit of the UAV-BS network with backhaul constraint and different user QoS requirements and demonstrate the importance and necessity of the joint bandwidth, power and trajectory optimization in maximizing the minimum user rate. Moreover, the obtained results provide design guidelines for the considered UAV-BS network.

The remainder of this paper is organized as follows. Section II presents the system model and problem formulation. Section III presents the proposed joint bandwidth, power and trajectory optimization algorithm. Section IV provides simulation results to verify the performance of the proposed algorithm. Finally, Section V concludes this paper.

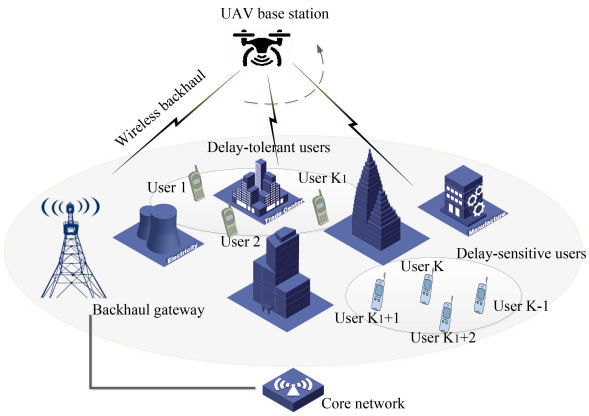

FIGURE 1. A UAV-BS network with backhaul constraint and different user QoS requirements.

II. SYSTEM MODEL AND PROBLEM FORMULATION

A. SYSTEM MODEL

As shown in Fig. 1, we consider a UAV-BS-assisted wireless communication network where an aerial UAV-BS is serving K users on the ground. The user set is denoted by $\mathcal{K} \triangleq \{1, \ldots, K\}$. The UAV-BS connects to the core network via a backhaul gateway (BHG) on the ground, and the wireless link between the UAV-BS and the BHG is called the backhaul link. Without loss of generality, we focus on the downlink communication from the UAV-BS to the ground users, and the

study can be extended to the uplink communication scenario straightforwardly.

We use the Cartesian coordinate system to express location. The locations of the BHG and user k, $k \in \mathcal{K}$, are fixed at $[\mathbf{w}_{\mathrm{BH}}^T, 0]^T$ and $[\mathbf{w}_k^T, 0]^T$, respectively, where $\mathbf{w}_{\mathrm{BH}} = [x_0, y_0]^T \in \mathbb{R}^{2\times 1}$ and $\mathbf{w}_k = [x_k, y_k]^T \in \mathbb{R}^{2\times 1}$ denote their respective horizontal coordinates, and the superscript T denotes the transpose operation. The UAV-BS flies at a fixed altitude H in meter (m), and its coordinate at time t, $0 \le t \le T$, is $[\mathbf{s}^T(t), H]^T$, where $\mathbf{s}(t) = [x(t), y(t)]^T \in \mathbb{R}^{2\times 1}$ denotes its horizontal coordinate at time t, and T in second (s) denotes the flight period of the UAV-BS. For ease of deployment, we require that the UAV-BS returns to its initial departure location at the end of the flight period, and denote its maximum speed by $V_{\max}$. Thus, the UAV-BS is subject to the following mobility constraints

$$\mathbf{s}(0) = \mathbf{s}(T), \tag{1}$$

$$\| \dot{\mathbf{s}}(t) \| \le V_{\max}, \quad 0 \le t \le T. \tag{2}$$

The trajectory of the UAV-BS $\{\mathbf{s}(t) | 0 \le t \le T\}$ is continuous over time t, so optimizing it involves infinite number of variables and is thus difficult. To facilitate trajectory optimization, we discretize the trajectory by dividing the flight period T into N time slots with equal length, and approximate the trajectory by using the sequence $\{\mathbf{s}_n, 0 \le n \le N\}$, where $\mathbf{s}_n = [x_n, y_n]^T$ denotes the horizontal coordinate of the UAV-BS at time slot n. The number of time slot N is sufficiently large such that the length of each time slot $\xi_t = T/N$ is small enough. As a result, the UAV-BS can be regarded as static by the users on the ground at each time slot. Thus, the mobility constraints of the UAV, i.e., (1) and (2), can be approximately written as

$$\mathbf{s}_0 = \mathbf{s}_N, \tag{3}$$

$$\| \mathbf{s}_{n+1} - \mathbf{s}_n \|^2 \le L_{\max}^2, \quad n = 0, \ldots, N-1, \tag{4}$$

where $L_{\max} \triangleq V_{\max}\xi_t$ is the maximum distance that the UAV-BS can fly within each time slot. Then, the distance between the UAV-BS and user k, $k \in \mathcal{K}$, and that between the UAV-BS and the BHG at time slot n can be written as

$$d_{k,n} = \sqrt{H^2 + \| \mathbf{s}_n - \mathbf{w}_k \|^2}, \tag{5}$$

and

$$d_{\mathrm{BH},n} = \sqrt{H^2 + \| \mathbf{s}_n - \mathbf{w}_{\mathrm{BH}} \|^2}, \tag{6}$$

respectively.

Since measurement results show that the channel between a UAV above ground and a node on the ground is dominated by the LoS link [25], the free-space propagation model offers a good approximation for the channels between the UAV-BS and all ground users and that between the UAV-BS and the BHG. Thus, the channel power gain between the UAV-BS and user k, $k \in \mathcal{K}$, at time slot n can be written as

$$\varphi_{k,n} = \frac{\beta_0}{d_{k,n}^2} = \frac{\beta_0}{H^2 + \| \mathbf{s}_n - \mathbf{w}_k \|^2}, \tag{7}$$

where β_0 is denoted as the channel power gain of a wireless channel at the reference distance $d_0 = 1$ m. Similarly, the channel power gain between the UAV-BS and the BHG at time slot n can be written as

$$\varphi_{\mathrm{BH},n} = \frac{\beta_0}{d_{\mathrm{BH},n}^2} = \frac{\beta_0}{H^2 + \| \mathbf{s}_n - \mathbf{w}_{\mathrm{BH}} \|^2}. \tag{8}$$

We assume that there is no dedicated spectrum for the backhaul link in the considered UAV-BS network due to spectrum scarcity. Thus, the in-band backhaul scheme is applied, which lets the backhaul link and the data links share the same spectrum with bandwidth B in Hertz (Hz). In order to avoid interference, different links are allocated with orthogonal spectrum. Denote the bandwidth portions of the backhaul link and the data link from the UAV-BS to user k at time slot n by $x_{0,n}$ and $x_{k,n}$, respectively, and they should satisfy the following bandwidth constraints

$$\sum_{k=0}^{K} x_{k,n} \le 1, \quad \forall n, \tag{9a}$$

$$0 \le x_{k,n} \le 1, \quad \forall n,\ k \in \{0\} \cup \mathcal{K}. \tag{9b}$$

Suppose that the UAV-BS transmits signal to user k with power $p_{k,n}$ at time slot n, and $p_{k,n}$ is subject to a total power constraint and a non-negative constraint as follows

$$\sum_{k=1}^{K} p_{k,n} \le p_{\max}, \quad \forall n, \tag{10a}$$

$$p_{k,n} \ge 0, \quad \forall n, k, \tag{10b}$$

where $p_{\max}$ denotes the maximum total power of the UAV-BS. Thus, the achievable data rate of user k at time slot n in bit per second per Hertz (bps/Hz) can be expressed as

$$\begin{aligned} R_{k,n} &= x_{k,n} \log_2 \left(1 + \frac{p_{k,n}\varphi_{k,n}}{x_{k,n}BN_0}\right) \\ &= x_{k,n} \log_2 \left(1 + \frac{p_{k,n}\zeta_0}{x_{k,n}\lambda_{k,n}}\right), \end{aligned} \tag{11}$$

where N_0 denotes the power spectral density of the additive white Gaussian noise at the receiver, $\zeta_0 = \frac{\beta_0}{BN_0}$, and $\lambda_{k,n} = H^2 + \| \mathbf{s}_n - \mathbf{w}_k \|^2$. We suppose that the BHG transmits signal to the UAV-BS with a constant power p_{b}, and express the achievable data rate of the backhaul link at time slot n as

$$\begin{aligned} R_{\mathrm{BH},n} &= x_{0,n} \log_2 (1 + \frac{p_{\mathrm{b}}\varphi_{\mathrm{BH},n}}{x_{0,n}BN_0}) \\ &= x_{0,n} \log_2 (1 + \frac{p_{\mathrm{b}}\zeta_0}{x_{0,n}\lambda_{\mathrm{BH},n}}), \end{aligned} \tag{12}$$

where $\lambda_{\mathrm{BH},n} = H^2 + \| \mathbf{s}_n - \mathbf{w}_{\mathrm{BH}} \|^2$. Since the UAV-BS can only transmit the data received from the core network (via the BHG) to the users, the sum rate of all users should be no greater than the rate of the backhaul link at any time slot, which is called the backhaul rate constraint and is written as

$$R_{\mathrm{BH},n} \ge \sum_{k=1}^{K} R_{k,n}, \ \forall n. \tag{13}$$

The users in the network have different QoS requirements. Among them, K_1 users are delay-tolerant users, whose set is defined as $\mathcal{K}_1 \triangleq \{1, \ldots, K_1\}$, and the remaining $K - K_1$ users are delay-sensitive users, whose set is defined as $\mathcal{K}_2 \triangleq \{K_1 + 1, \ldots, K\}$. The delay-tolerant users require non-real-time data traffic service and are tolerant to delay, while the delay-sensitive users require real-time data traffic service (e.g., data streaming) and need to avoid communication delay. To guarantee no delay, the data rates of the delay-sensitive users should be no smaller than a minimum rate requirement value $R_{\min}$ at any time, i.e.,

$$R_{k,n} \geq R_{\min}, \quad k \in \mathcal{K}_2, \ \forall n. \tag{14}$$

Here, $R_{\min}$ is determined by the QoS requirement of the delay-sensitive users.

B. PROBLEM FORMULATION

To improve the data rate of the delay-tolerant users and guarantee the QoS requirement of the delay-sensitive users, we aim to maximize the minimum average rate of the delay-tolerant users, i.e., $\min_{k\in\mathcal{K}_1} \frac{1}{N}\sum_{n=1}^{N} R_{k,n}$, by jointly optimizing the bandwidth portions of the backhaul link and all data links $\mathbf{X} \triangleq \{x_{k,n}, \forall n, k \in \{0\} \cup \mathcal{K}\}$,[1] the transmit power allocated to all users $\mathbf{P} \triangleq \{p_{k,n}, \forall n, k \in \mathcal{K}\}$, and the trajectory of the UAV-BS $\mathbf{S} \triangleq \{\mathbf{s}_n, \forall n\}$, subject to the mobility constraints of the UAV-BS in (3) and (4), the bandwidth constraints in (9), the transmit power constraints in (10), the backhaul rate constraint in (13), and the minimum rate constraint of the delay-sensitive users in (14). By introducing a slack variable ς to denote the minimum average rate of the delay-tolerant users, we formulate the problem as[2]

$$\text{(P1)}: \max_{\varsigma,\mathbf{X},\mathbf{P},\mathbf{S}} \ \varsigma \tag{15a}$$

$$\text{s.t.} \ \frac{1}{N}\sum_{n=1}^{N} R_{k,n} \geq \varsigma, \quad k \in \mathcal{K}_1, \tag{15b}$$

$$(3), (4), (9), (10), (13), (14). \tag{15c}$$

Since the left-hand-sides (LHSs) of constraints (13) and (14) are non-concave with respect to $\mathbf{X}$, $\mathbf{P}$, and $\mathbf{S}$, and the right-hand-side (RHS) of constraint (13) are non-convex with respect to $\mathbf{X}$, $\mathbf{P}$, and $\mathbf{S}$, problem (P1) is a non-convex optimization problem. Furthermore, problem (P1)'s optimization variables couple together in the constraints, so the problem is difficult to solve. Nevertheless, we propose an efficient algorithm to solve find high-quality suboptimal solution to it as follows.

III. PROPOSED ALGORITHM FOR PROBLEM (P1)

To resolve the variable coupling issue, we apply the alternating optimization method to solve problem (P1). First, the proposed algorithm partitions all optimization variables into two blocks, where the first block includes the bandwidth portion variables $\mathbf{X}$ and the transmit power variables $\mathbf{P}$, and the second block includes the UAV trajectory variables $\mathbf{S}$. Next, with such variable partition, problem (P1) can be divided into two subproblems, denoted as subproblems 1 and 2. Subproblem 1 optimizes variables $\mathbf{X}$ and $\mathbf{P}$ under fixed variables $\mathbf{S}$, while subproblem 2 optimizes variables $\mathbf{S}$ under fixed variables $\mathbf{X}$ and $\mathbf{P}$. The proposed algorithm solves subproblems 1 and 2 alternatively and iteratively until the objective value of problem (P1) converges. In the following, the proposed methods for solving subproblems 1 and 2 will be presented, respectively. Then, the overall proposed algorithm will be summarized.

A. BANDWIDTH AND TRANSMIT POWER OPTIMIZATION UNDER FIXED UAV TRAJECTORY

We first deal with subproblem 1, which optimizes the bandwidth and transmit power allocation of the UAV-BS network, i.e., $\mathbf{X}$ and $\mathbf{P}$, with fixed UAV trajectory $\mathbf{S}$. We let $f_{k,n} = \frac{\zeta_0}{\lambda_{k,n}}$ and $f_{\text{BH},n} = \frac{\zeta_0}{\lambda_{\text{BH},n}}$, and formulate the problem as

$$\text{(P2)}: \max_{\varsigma,\mathbf{X},\mathbf{P}} \ \varsigma \tag{16a}$$

$$\text{s.t.} \ \frac{1}{N}\sum_{n=1}^{N} x_{k,n}\log_2\left(1+\frac{p_{k,n}f_{k,n}}{x_{k,n}}\right) \geq \varsigma, \quad k \in \mathcal{K}_1,$$

$$x_{0,n}\log_2\left(1+\frac{p_{\text{h}}f_{\text{BH},n}}{x_{0,n}}\right) \tag{16b}$$

$$\geq \sum_{k=1}^{K} x_{k,n}\log_2\left(1+\frac{p_{k,n}f_{k,n}}{x_{k,n}}\right), \quad \forall n, \tag{16c}$$

$$x_{k,n}\log_2\left(1+\frac{p_{k,n}f_{k,n}}{x_{k,n}}\right) \geq R_{\min}, \quad k \in \mathcal{K}_2, \ \forall n, \tag{16d}$$

$$(9), (10), \tag{16e}$$

where constraints (16c) and (16d) are from (13) and (14), respectively. Since the RHS of constraint (16c) is concave with respect to $x_{k,n}$ and $p_{k,n}$, problem (P2) is non-convex and cannot be solved by standard optimization techniques. To solve problem (P2), we introduce slack variables $\mathbf{u} \triangleq \{u_{k,n}, \forall k, n\}$ to it, and formulate the following problem.

$$\text{(P3)}: \max_{\varsigma,\mathbf{X},\mathbf{P},\mathbf{u}} \ \varsigma \tag{17a}$$

$$\text{s.t.} \ \frac{1}{N}\sum_{n=1}^{N} u_{k,n} \geq \varsigma, \quad k \in \mathcal{K}_1, \forall n, \tag{17b}$$

$$x_{0,n}\log_2\left(1+\frac{p_{\text{h}}f_{\text{BH},n}}{x_{0,n}}\right) \geq \sum_{k=1}^{K} u_{k,n}, \quad \forall n, \tag{17c}$$

$$u_{k,n} \geq R_{\min}, \quad k \in \mathcal{K}_2, \ \forall n, \tag{17d}$$

$$u_{k,n} \leq x_{k,n}\log_2\left(1+\frac{p_{k,n}f_{k,n}}{x_{k,n}}\right), \quad \forall k, n, \tag{17e}$$

$$(9), (10). \tag{17f}$$

[1] Optimizing the bandwidth portion over all links and all time slots can be regarded as a generalized case of optimizing user association in [3].

[2] In general, the altitude of the UAV-BS H can also be optimized subject to the constraints of minimum and maximum allowable altitudes. However, it is easy to verify that the minimum altitude can always achieve the optimal value of our considered problem under the LoS air-to-ground channel model.

It can be shown that problem (P3) and problem (P2) have the same optimal solution on $\mathbf{X}$ and $\mathbf{P}$. To see that, we prove that there exists an optimal solution to problem (P3) that satisfies constraint (17e) with equality. By contradiction, we assume that $x_{j,m}$ and $p_{j,m}$ are an optimal solution to problem (P3), for some $j \in \mathcal{K}$ and $m \in \{1, \ldots, N\}$, such that constraint (17e) is satisfied with strict inequality. Then, based on $x_{j,m}$ and $p_{j,m}$, we can always find another solution to problem (P3), namely $\tilde{x}_{j,m}$ and $\tilde{p}_{j,m}$, with $\tilde{x}_{j,m} \leq x_{j,m}$ and $\tilde{p}_{j,m} \leq p_{j,m}$, which lower the value of the RHS of constraint (17e) to make its equality hold. Since $\tilde{x}_{j,m}$ and $\tilde{p}_{j,m}$ do not decrease the objective value of problem (P3), they are also an optimal solution to problem (P3). Furthermore, when constraint (17e) is satisfied with equality, problems (P3) and (P2) are equivalent, so they have the same optimal solution on $\mathbf{X}$ and $\mathbf{P}$. Hence, we can obtain the solution on $\mathbf{X}$ and $\mathbf{P}$ in problem (P2) by solving problem (P3). Since the objective function (17a), constraints (17b), (17d), and (17f) are linear, and the LHS of constraint (17c) and the RHS of constraint (17e) are concave with respect to $\mathbf{X}$ and $\mathbf{P}$, problem (P3) is a convex optimization problem. We solve it by using the interior-point method [26].

B. UAV TRAJECTORY OPTIMIZATION UNDER FIXED BANDWIDTH AND TRANSMIT POWER

Now, we deal with subproblem 2, which optimizes the trajectory of the UAV-BS with fixed bandwidth and transmit power allocation. By letting $g_{k,n} = \frac{p_{k,n}\zeta_0}{x_{k,n}}$ and $g_{0,n} = \frac{p_{\mathrm{ap},n}\zeta_0}{x_{0,n}}$, we formulate the problem as

$$
\begin{aligned}
(\mathrm{P4}): \max_{\varsigma,\mathbf{S}} \ & \varsigma && (18a)\\
\text{s.t. } & \frac{1}{N}\sum_{n=1}^{N} x_{k,n}\log_2\left(1+\frac{g_{k,n}}{H^2+\parallel \mathbf{s}_n-\mathbf{w}_k\parallel^2}\right) \\
& \geq \varsigma, \quad k\in\mathcal{K}_1, && (18b)\\
& x_{0,n}\log_2\left(1+\frac{g_{0,n}}{H^2+\parallel \mathbf{s}_n-\mathbf{w}_{\mathrm{BH}}\parallel^2}\right) \\
& \geq \sum_{k=1}^{K} x_{k,n}\log_2\left(1+\frac{g_{k,n}}{H^2+\parallel \mathbf{s}_n-\mathbf{w}_k\parallel^2}\right), \\
& \forall n, && (18c)\\
& x_{k,n}\log_2\left(1+\frac{g_{k,n}}{H^2+\parallel \mathbf{s}_n-\mathbf{w}_k\parallel^2}\right)\geq R_{\min}, \\
& k\in\mathcal{K}_2, \quad \forall n, && (18d)\\
& (3), (4), && (18e)
\end{aligned}
$$

where constraints (18c) and (18d) are from (13) and (14), respectively. Note that (18b), (18c) and (18d) are non-convex constraints, problem (P4) is a non-convex optimization problem and difficult to solve optimally. As a compromise alternative, we solve it suboptimally, and the method is presented as follows.

First, we introduce slack variables $\mathbf{l} \triangleq \{l_{k,n}, \ \forall k, n\}$ to problem (P4), and formulate the following problem:

$$
\begin{aligned}
(\mathrm{P5}): \max_{\varsigma,\mathbf{S},\mathbf{l}} \ & \varsigma && (19a)\\
\text{s.t. } & \frac{1}{N}\sum_{n=1}^{N} l_{k,n}\geq\varsigma, \quad k\in\mathcal{K}_1, && (19b)\\
& x_{0,n}\log_2\left(1+\frac{g_{0,n}}{H^2+\parallel \mathbf{s}_n-\mathbf{w}_{\mathrm{BH}}\parallel^2}\right)\geq\sum_{k=1}^{K} l_{k,n}, \\
& \forall n, && (19c)\\
& l_{k,n}\geq R_{\min}, \quad k\in\mathcal{K}_2, \ \forall n, && (19d)\\
& l_{k,n}\leq x_{k,n}\log_2\left(1+\frac{g_{k,n}}{H^2+\parallel \mathbf{s}_n-\mathbf{w}_k\parallel^2}\right), \\
& \forall k, n, && (19e)\\
& (3), (4). && (19f)
\end{aligned}
$$

Similar to showing that problems (P3) and (P2) have the same optimal solution on $\mathbf{X}$ and $\mathbf{P}$, we can show that there exists an optimal solution to problem (P5) such that constraint (19e) is satisfied with equality, and thus problem (P5) and problem (P4) have the same solution on $\mathbf{S}$. Therefore, we can obtain the solution to $\mathbf{S}$ by solving problem (P5). However, problem (P5) is still difficult to solve optimally since the LHS of (19c) and the RHS of (19e) are non-concave with respect to $\mathbf{s}_n$.

Next, we focus on solving problem (P5) approximately by using the successive convex approximation technique, which is iterative. Specifically, in each iteration, the successive convex optimization technique assumes an initial point and obtains an approximate solution to problem (P5) by maximizing the objective function of problem (P5) within a convex feasible region, which is constructed by using the initial point. The obtained approximate solution in the current iteration will be used as the initial point in the next iteration. The iteration process stops when the objective value of problem (P5) convergences.

We present the details as follows. Without loss of generality, we assume that $\mathbf{S}^{(r)} \triangleq \{\mathbf{s}_n^{(r)}, \forall n\}$ is the obtained UAV trajectory solution in the r-th iteration, $r \geq 0$. In the $(r+1)$-th iteration, we use $\mathbf{S}^{(r)}$ as the initial point and find the approximate solution as follows. Note that although the LHS of (19c) and the RHS of (19e) are not concave with respect to $\mathbf{s}_n$, they are convex with respect to $\parallel \mathbf{s}_n - \mathbf{w}_{\mathrm{BH}} \parallel^2$ and $\parallel \mathbf{s}_n - \mathbf{w}_k \parallel^2$, respectively. Thus, we construct lower bounds of the LHS of (19c) and the RHS of (19e) by using their first-order Taylor expansion at $\parallel \mathbf{s}_n^{(r)} - \mathbf{w}_{\mathrm{BH}} \parallel^2$ and $\parallel \mathbf{s}_n^{(r)} - \mathbf{w}_k \parallel^2$, denoted by $R_{\mathrm{BH},n}^{\mathrm{lb},(r)}$ and $R_{k,n}^{\mathrm{lb},(r)}$, respectively, which are expressed as

$$
\begin{aligned}
& x_{0,n}\log_2\left(1+\frac{g_{0,n}}{H^2+\parallel \mathbf{s}_n-\mathbf{w}_{\mathrm{BH}}\parallel^2}\right) \\
& \geq -\eta_{\mathrm{BH},n}^{(r)}\left(\parallel \mathbf{s}_n-\mathbf{w}_{\mathrm{BH}}\parallel^2-\parallel \mathbf{s}_n^{(r)}-\mathbf{w}_{\mathrm{BH}}\parallel^2\right)+\phi_{\mathrm{BH},n}^{(r)} \\
& \triangleq R_{\mathrm{BH},n}^{\mathrm{lb},(r)}, && (20)\\
& x_{k,n}\log_2\left(1+\frac{g_{k,n}}{H^2+\parallel \mathbf{s}_n-\mathbf{w}_k\parallel^2}\right) \\
& \geq -\eta_{k,n}^{(r)}\left(\parallel \mathbf{s}_n-\mathbf{w}_k\parallel^2-\parallel \mathbf{s}_n^{(r)}-\mathbf{w}_k\parallel^2\right)+\phi_{k,n}^{(r)} \\
& \triangleq R_{k,n}^{\mathrm{lb},(r)}, && (21)
\end{aligned}
$$

where

$$\eta_{\mathrm{BH},n}^{(r)} = \frac{x_{0,n} g_{0,n} \log_2(e)}{\lambda_{\mathrm{BH},n}^{(r)} (\lambda_{\mathrm{BH},n}^{(r)} + g_{0,n})},$$
$$\phi_{\mathrm{BH},n}^{(r)} = x_{0,n} \log_2\left(1 + \frac{g_{0,n}}{\lambda_{\mathrm{BH},n}^{(r)}}\right),$$
$$\lambda_{\mathrm{BH},n}^{(r)} = H^2 + \| \mathbf{s}_n^{(r)} - \mathbf{w}_{\mathrm{BH}} \|^2,$$
$$\eta_{k,n}^{(r)} = \frac{x_{k,n} g_{k,n} \log_2(e)}{\lambda_{k,n}^{(r)} (\lambda_{k,n}^{(r)} + g_{k,n})}$$
$$\phi_{k,n}^{(r)} = x_{k,n} \log_2\left(1 + \frac{g_{k,n}}{\lambda_{k,n}^{(r)}}\right),$$
$$\lambda_{k,n}^{(r)} = H^2 + \| \mathbf{s}_n^{(r)} - \mathbf{w}_k \|^2 .$$

Then, by replacing the LHS of (19c) and the RHS of (19e) with $R_{\mathrm{BH},n}^{\mathrm{lb},(r)}$ and $R_{k,n}^{\mathrm{lb},(r)}$, respectively, we formulate the following approximate problem of (P5):

$$(\mathrm{P6}): \quad \max_{\varsigma, \mathbf{S}, \mathbf{l}} \ \varsigma \tag{22a}$$
$$\text{s.t.} \ \frac{1}{N} \sum_{n=1}^{N} l_{k,n} \geq \varsigma, \quad k \in \mathcal{K}_1, \tag{22b}$$
$$R_{\mathrm{BH},n}^{\mathrm{lb},(r)} \geq \sum_{k=1}^{K} l_{k,n}, \ \forall n, \tag{22c}$$
$$l_{k,n} \geq R_{\min}, \quad k \in \mathcal{K}_2, \forall n, \tag{22d}$$
$$l_{k,n} \leq R_{k,n}^{\mathrm{lb},(r)}, \quad \forall k, n, \tag{22e}$$
$$(3), (4). \tag{22f}$$

Since the LHS of constraint (22c) and the RHS of constraint (22e) are concave with respect to $\mathbf{s}_n$ and the other constraints are linear, the feasible region of problem (P6) is convex. In addition, the objective function of problem (P6) is linear, so problem (P6) is a convex optimization problem, and the interior-point method can be applied to obtain the optimal solution to it [26].

Since $R_{\mathrm{BH},n}^{\mathrm{lb},(r)}$ and $R_{k,n}^{\mathrm{lb},(r)}$ are the lower bounds of the LHS of (19c) and the RHS of (19e), respectively, constraints (22c) and (22e) imply constraints (19c) and (19e), respectively. Thus, the solution obtained by solving problem (P6) is a feasible solution to problem (P5). Furthermore, since in the $(r+1)$-th iteration, the solution $\mathbf{S}^{(r+1)}$ is an optimal solution to problem (P6) and the initial point $\mathbf{S}^{(r)}$ is within the feasible region, the objective value of problem (P5) with $\mathbf{S}^{(r+1)}$ is no smaller than that with $\mathbf{S}^{(r)}$. Therefore, the objective value of problem (P5) is non-decreasing over iterations.

C. OVERALL PROPOSED ALGORITHM

We summarized the proposed algorithm in Algorithm 1, where $f(\mathbf{X}, \mathbf{P}, \mathbf{S})$ denotes the objective value of problem (P1) with solution $\mathbf{X}$, $\mathbf{P}$, and $\mathbf{S}$, and $\eta > 0$ and $\tau > 0$ denote thresholds indicating the convergence accuracy. As analysis in the previous subsections, the objective value of problem (P1) with solution obtained by executing steps 4-10 of Algorithm 1 is non-decreasing over iterations. Furthermore, since the objective value is upper bounded by a finite value, Algorithm 1 is guaranteed to converge. In addition, the computational complexity of Algorithm 1 is mainly due to step 4 and steps 6-10, whose complexities are $\mathcal{O}[(KN)^{3.5}]$ and $\mathcal{O}[N_1(KN)^{3.5}]$ [26], [27], respectively, where N_1 is the iteration number of steps 6-10. As a result, the computational complexity of Algorithm 1 is $\mathcal{O}[N_{\mathrm{ite}}(N_1+1)(KN)^{3.5}]$, where N_{ite} denotes the iteration number from step 2 to step 12.

Algorithm 1 Proposed Algorithm for Problem (P1)

1: Initialization: Obtain an initial solution $\mathbf{X}^{(0)}$, $\mathbf{P}^{(0)}$, and $\mathbf{S}^{(0)}$; Calculate $\varsigma^{(0)} = f(\mathbf{X}^{(0)}, \mathbf{P}^{(0)}, \mathbf{S}^{(0)})$; Set $l = 0$.
2: **repeat**
3: Update $l = l + 1$.
4: With fixed trajectory $\mathbf{S}^{(l-1)}$, update the bandwidth variable $\mathbf{X}^{(l)}$ and transmit power variable $\mathbf{P}^{(l)}$ by solving problem (P3).
5: With fixed bandwidth $\mathbf{X}^{(l)}$ and transmit power $\mathbf{P}^{(l)}$, update the trajectory $\mathbf{S}^{(l)}$ in the following iteration process: Set $\tilde{\mathbf{S}}^{(0)} = \mathbf{S}^{(l-1)}$ and $r = 0$; Calculate $\zeta^{(0)} = f(\mathbf{X}^{(l)}, \mathbf{P}^{(l)}, \tilde{\mathbf{S}}^{(0)})$.
6: **repeat**
7: Update $r = r + 1$.
8: With $\tilde{\mathbf{S}}^{(r-1)}$ as initial point, solve problem (P6) and denote the obtained solution by $\tilde{\mathbf{S}}^{(r)}$.
9: Calculate $\zeta^{(r)} = f(\mathbf{X}^{(l)}, \mathbf{P}^{(l)}, \tilde{\mathbf{S}}^{(r)})$.
10: **until** $\frac{|\zeta^{(r)} - \zeta^{(r-1)}|}{|\zeta^{(r-1)}|} < \eta$. Set $\mathbf{S}^{(l)} = \tilde{\mathbf{S}}^{(r)}$.
11: Calculate $\varsigma^{(l)} = f(\mathbf{X}^{(l)}, \mathbf{P}^{(l)}, \mathbf{S}^{(l)})$.
12: **until** $\frac{|\varsigma^{(l)} - \varsigma^{(l-1)}|}{|\varsigma^{(l-1)}|} < \tau$.

IV. SIMULATION RESULTS

In this section, we present computer simulation results to verify the performance of our proposed joint bandwidth, power and trajectory optimization algorithm (denoted by "Joint"), as compared to the following benchmark schemes.

- Trajectory optimization with fixed bandwidth and power allocation scheme (denoted by "T-Opt"): it fixes the bandwidths of different links and the power allocated to different users by setting $x_{0,n} = 1/2$, $x_{k,n} = 1/(2K)$, and $p_{k,n} = p_{\max}/K$, and optimizes the UAV trajectory by executing steps 5-10 of Algorithm 1.
- Power and trajectory optimization with fixed bandwidth scheme (denoted by "P-T-Opt"): it fixes the bandwidths of the backhaul and data links by setting $x_{0,n} = 1/2$ and $x_{k,n} = 1/(2K)$, and optimizes the transmit power and UAV trajectory by using an alternating optimization algorithm similar to Algorithm 1.
- Bandwidth and power optimization with circular trajectory scheme (denoted by "B-P-Opt-Circle-T"): it applies a traditional circular trajectory [28] and optimizes the bandwidth and power by executing step 4 of Algorithm 1. The circular trajectory is generated as follows. We denote the

center and radius of the trajectory by $\mathbf{c}_t = [x_t, y_t]^T$ and r_t, respectively. We set $\mathbf{c}_t = \mathbf{w}_{\rm BH}$. Under the given maximum speed of the UAV $V_{\max}$ and flight duration T, r_t is upper bounded by

$$r_t \le r_{\max} = \frac{V_{\max} T}{2\pi}. \tag{23}$$

Furthermore, to avoid the UAV from flying too far away from the users, we also set the following upper bound

$$r_t \le \max_k r_k = \max_k \|\mathbf{w}_k - \mathbf{w}_{\rm BH}\|. \tag{24}$$

Thus, we set $r_t = \min(r_{\max}, \max_k r_k)$. Therefore, the circular trajectory is set as $\mathbf{S}^{(0)} = \{\mathbf{s}_n^{(0)},\ n = 1, \ldots, N\}$, where

$$\mathbf{s}_n^{(0)} = [x_t - r_t \cos\alpha_n, y_t - r_t \sin\alpha_n]^T. \tag{25}$$

Here, $\alpha_n = 2\pi \frac{(n-1)}{N-1}$. This circular trajectory is also used for the initial trajectory of the other schemes.

In the simulations, we set that the ground users randomly locate in an area with a size 2×2 km^2. There are $K = 6$ users, where users 1 and 2 are delay-sensitive users, and users 3-6 are delay-tolerant users. To compare the proposed and benchmark schemes, the following results are obtained from one random realization of users' locations. The flying altitude and maximum speed of the UAV-BS are $H = 100$ m and $V_{\max} = 50$ m/s, respectively. The total bandwidth of the network spectrum is set as $B = 10$ MHz. The maximum total transmit power of the UAV-BS and the transmit power of the BHG are set as $p_{\max} = 2$ W and $p_{\rm b} = 2$ W, respectively. The other parameters are set as $\beta_0 = -60$ dB, $N_0 = -169$ dBm/Hz, $\tau = 10^{-4}$, and $\eta = 10^{-4}$.

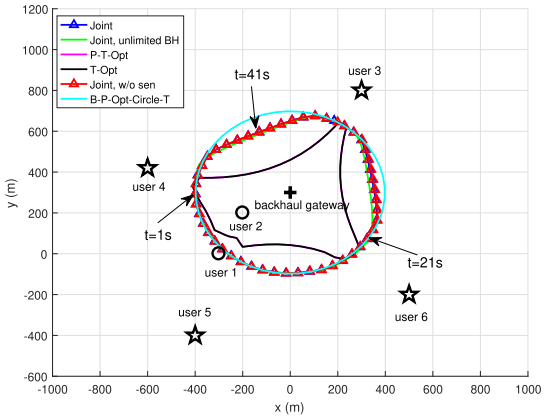

FIGURE 2. UAV trajectories optimized by different schemes when $T = 50$ s and $R_{\min} = 0.5$ bps/Hz, where makers '+', 'o', and '⋆' indicate the locations of the BHG, delay-sensitive users, and delay-tolerant users, respectively.

Figs. 2 and 3 show the UAV trajectories obtained by different schemes when the flight periods of the UAV are $T = 50$ s and $T = 120$ s, respectively, with the minimum rate requirement of the delay-sensitive users $R_{\min} = 0.5$ bps/Hz. The UAV trajectories of two ideal scenarios are also shown. One ideal scenario is that the UAV-BS network has a backhaul link with unlimited bandwidth, where we jointly optimize the bandwidth, transmit power, and the UAV trajectory without

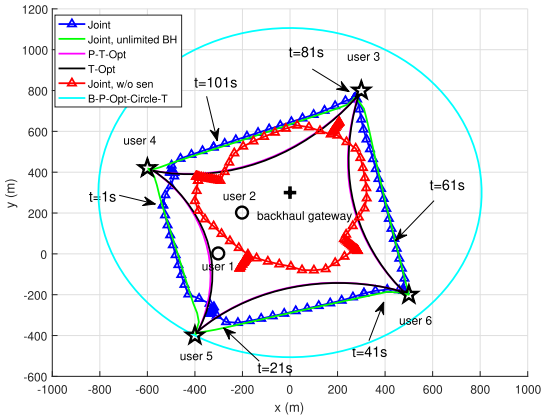

FIGURE 3. UAV trajectories optimized by different schemes when $T = 120$ s and $R_{\min} = 0.5$ bps/Hz, where makers '+', 'o', and '⋆' indicate the locations of the BHG, delay-sensitive users, and delay-tolerant users, respectively.

the backhaul link constraint. The other ideal scenario is that the network has no delay-sensitive users, where we jointly optimize the bandwidth, transmit power, and the UAV trajectory without the minimum rate requirement of delay-sensitive users. The joint optimization algorithms used in the former and latter ideal scenarios are both similar to Algorithm 1, and their obtained results are denoted by "Joint, unlimited BH" and "Joint, w/o sen", respectively. In Fig. 2, it is observed that the UAV trajectories optimized by all schemes are similar, except the "T-Opt" and "P-T-Opt" schemes. This is because when $T = 50$ s, all schemes have limited degree of freedom for trajectory optimization.

In Fig. 3, It is observed that when $T = 120$ s, there is more degree of freedom for trajectory optimization, the UAV trajectories obtained by different schemes are different. In the unlimited backhaul bandwidth scenario, the UAV-BS travels from one delay-tolerant user to another delay-tolerant user in straight lines and hovers on top of each delay-tolerant user for some time. Unlike this ideal scenario, when the backhaul link connecting the UAV-BS and the BHG is limited, the proposed "Joint" algorithm does not let the UAV-BS reach the point on top of each delay-tolerant user, and it lets the UAV-BS remain static at a point near the delay-tolerant user being served for some time. In this way, the proposed algorithm can balance the data links and the backhaul link's data transmission amounts. In the no delay-sensitive user scenario, the UAV-BS does not stay static when serving a delay-tolerant user but flies in slow speed in a line that connects the BHG and the delay-tolerant user, and the distance between the UAV-BS and the BHG is much lower than the other schemes. This is because in the ideal no delay-sensitive user scenario, the UAV-BS can be regarded as a relay between the BHG and the serving users, thus the result of this ideal scenario is consistent with that in the UAV relaying communication [4]. It is also observed that the trajectories obtained by the "P-T-Opt" and "T-Opt" schemes are similar: the UAV-BS flies from one delay-tolerant user to another delay-tolerant user in an

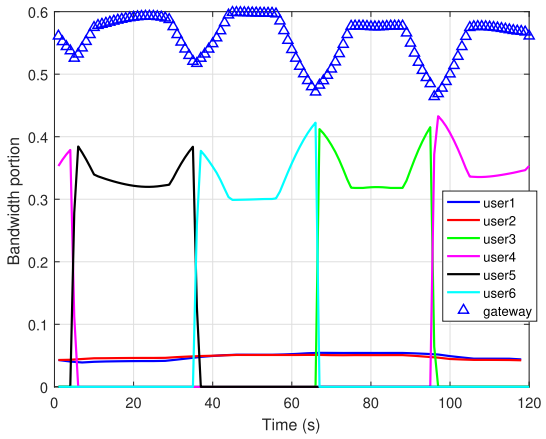

FIGURE 4. Bandwidth portions of different data links obtained by the proposed algorithm versus time ($T = 120$ s, $R_{\min} = 0.5$ bps/Hz).

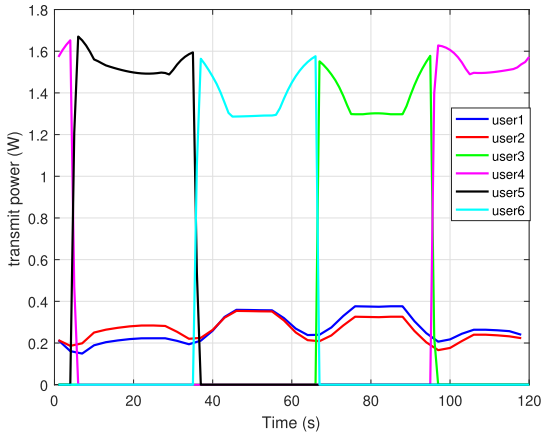

FIGURE 5. Transmit power allocated to different users obtained by the proposed algorithm versus time ($T = 120$ s, $R_{\min} = 0.5$ bps/Hz).

arc path that keeps it close to the delay-sensitive users at the same time. This is because in the "P-T-Opt" and "T-Opt" schemes, the bandwidths allocated to all links are fixed, thus the UAV-BS can only adjust its trajectory to guarantee the minimum rate requirement of the delay-sensitive users and to maximize the rate of the delay-tolerant at the same time.

Figs. 4 and 5 show the corresponding bandwidth portions allocated to different data links and transmit powers allocated to different users obtained by the proposed algorithm versus time, whose parameters are the same with that of Fig. 3. It can be observed that the delay-sensitive users, i.e., users 1 and 2, are always allocated with non-zero bandwidth and transmit power, so their minimum rate requirement can be satisfied at each time slot. In Fig. 4, it is observed that the bandwidth allocated to the backhaul link is also non-zero at all time slots, this is because the rate of the backhaul link should be no smaller than the sum of user rates at any time. In Figs. 4 and 5, it is observed that the delay-tolerant users are successively allocated with non-zero bandwidth and power, which means the UAV-BS only serves one delay-tolerant user at any time t and serves all of them successively over time. At each time slot, the sum of allocated bandwidth portions equals to

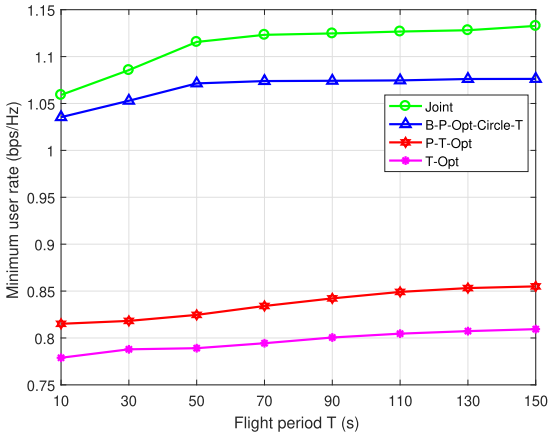

FIGURE 6. Minimum rates of the delay-tolerant users by different schemes versus flight period T ($R_{\min} = 0.5$ bps/Hz).

one strictly, and the sum of allocated transmit equals to the maximum total power, which is because the minimum user rate is maximized by using the total bandwidth and power.

Fig. 6 shows the minimum rates of the delay-tolerant users obtained by different schemes versus the UAV flight period T when $R_{\min} = 0.5$ bps/Hz. It is observed that the minimum rates of the delay-tolerant users obtained by all schemes increase with T. This is because with longer flight period T, more degree of freedom is available for the bandwidth, power, and trajectory optimization, and thus higher rate can be achieved. Furthermore, it is also observed that the minimum user rate of the proposed algorithm is significantly higher than that of the benchmark "B-P-Opt-Circle-T", "T-Opt" and "P-T-Opt" schemes. This is because the benchmark schemes do not fully use all available degree of freedom for optimization to improve the user rate. Besides, the "P-T-Opt" scheme only achieves a small rate gain over the "T-Opt" scheme, which shows that power allocation can only achieve marginal gain when the bandwidth allocation is fixed.

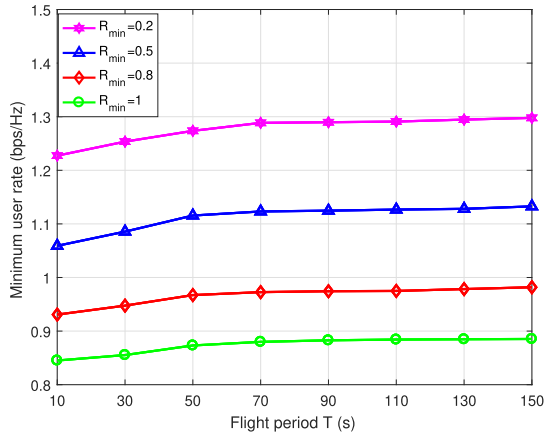

FIGURE 7. Minimum rates of the delay-tolerant users by the proposed algorithm versus flight period T with different values of $R_{\min}$.

Fig. 7 shows the minimum rates of the delay-tolerant users by the proposed algorithm versus T when $R_{\min}$ takes the

values of 0.2, 0.5, 0.8, and 1 bps/Hz. It can be observed that with $R_{\min}$ increasing, the minimum rate of the delay-tolerant users decreases. This is because higher $R_{\min}$ lets the network allocates more bandwidth and power to the delay-sensitive users and restricts the UAV-BS from getting closer to the delay-tolerant users, thus reduces the degree of freedom of the delay-tolerant users for bandwidth, power, and trajectory optimization.

V. CONCLUSION

In this paper, we investigate joint bandwidth, transmit power and trajectory optimization in a UAV-BS network with a bandwidth-limited backhaul link, where a part of the users are delay-tolerant and the other users are delay-sensitive. To guarantee the different QoS requirements of the users, we have proposed an efficient algorithm to maximize the minimum rate of the delay-tolerant users and satisfy the minimum rate requirement of the delay-sensitive users, by jointly optimizing the bandwidths of the backhaul link and the data links, the transmit powers allocated to the users, as well as the trajectory of the UAV-BS. Simulation results show that the proposed alternating optimization-based algorithm can achieve significantly higher minimum user rate performance, as compared to other benchmark schemes, which demonstrate that joint bandwidth, power, and trajectory optimization is essential for rate improvement in a UAV-BS network with the backhaul constraint and different user QoS requirements.

REFERENCES

[1] Y. Zeng, Q. Wu, and R. Zhang, "Accessing from the sky: A tutorial on UAV communications for 5G and beyond," *Proc. IEEE*, vol. 107, no. 12, pp. 2327–2375, Dec. 2019.

[2] Q. Wu, Y. Zeng, and R. Zhang, "Joint trajectory and communication design for UAV-enabled multiple access," in *Proc. IEEE Global Commun. Conf. (GLOBECOM)*, Dec. 2017, pp. 1–6.

[3] Q. Wu, Y. Zeng, and R. Zhang, "Joint trajectory and communication design for multi-UAV enabled wireless networks," *IEEE Trans. Wireless Commun.*, vol. 17, no. 3, pp. 2109–2121, Mar. 2018.

[4] Y. Zeng, R. Zhang, and T. J. Lim, "Throughput maximization for UAV-enabled mobile relaying systems," *IEEE Trans. Commun.*, vol. 64, no. 12, pp. 4983–4996, Dec. 2016.

[5] G. Zhang, H. Yan, Y. Zeng, M. Cui, and Y. Liu, "Trajectory optimization and power allocation for multi-hop UAV relaying communications," *IEEE Access*, vol. 6, pp. 48566–48576, 2018.

[6] Y. Huang, J. Xu, L. Qiu, and R. Zhang, "Cognitive UAV communication via joint trajectory and power control," in *Proc. IEEE 19th Int. Workshop Signal Process. Adv. Wireless Commun. (SPAWC)*, Jun. 2018, pp. 1–5.

[7] Z. Wang, L. Duan, and R. Zhang, "Adaptive deployment for UAV-aided communication networks," *IEEE Trans. Wireless Commun.*, vol. 18, no. 9, pp. 4531–4543, Sep. 2019.

[8] W. Mei, Q. Wu, and R. Zhang, "Cellular-connected UAV: Uplink association, power control and interference coordination," in *Proc. IEEE GLOBECOM*, Dec. 2018, pp. 206–212.

[9] S. Wang, M. Xia, and Y.-C. Wu, "Backscatter data collection with unmanned ground vehicle: Mobility management and power allocation," *IEEE Trans. Wireless Commun.*, vol. 18, no. 4, pp. 2314–2328, Apr. 2019.

[10] S. Wang, M. Xia, K. Huang, and Y.-C. Wu, "Wirelessly powered two-way communication with nonlinear energy harvesting model: Rate regions under fixed and mobile relay," *IEEE Trans. Wireless Commun.*, vol. 16, no. 12, pp. 8190–8204, Dec. 2017.

[11] P. Li and J. Xu, "Placement optimization for UAV-enabled wireless networks with multi-hop backhauls," *J. Commun. Inf. Netw.*, vol. 3, no. 4, pp. 64–73, Dec. 2018.

[12] M. Mozaffari, W. Saad, M. Bennis, and M. Debbah, "Unmanned aerial vehicle with underlaid device-to-device communications: Performance and tradeoffs," *IEEE Trans. Wireless Commun.*, vol. 15, no. 6, pp. 3949–3963, Jun. 2016.

[13] K. Li, W. Ni, X. Wang, R. P. Liu, S. S. Kanhere, and S. Jha, "Energy-efficient cooperative relaying for unmanned aerial vehicles," *IEEE Trans. Mobile Comput.*, vol. 15, no. 6, pp. 1377–1386, Jun. 2016.

[14] G. Zhang, Q. Wu, M. Cui, and R. Zhang, "Securing UAV communications via trajectory optimization," in *Proc. IEEE Global Commun. Conf. (GLOBECOM)*, Dec. 2017, pp. 1–6.

[15] G. Zhang, Q. Wu, M. Cui, and R. Zhang, "Securing UAV communications via joint trajectory and power control," *IEEE Trans. Wireless Commun.*, vol. 18, no. 2, pp. 1376–1389, Feb. 2019.

[16] M. Cui, G. Zhang, Q. Wu, and D. W. K. Ng, "Robust trajectory and transmit power design for secure UAV communications," *IEEE Trans. Veh. Technol.*, vol. 67, no. 9, pp. 9042–9046, Sep. 2018.

[17] Z. Yang, C. Pan, M. Shikh-Bahaei, W. Xu, M. Chen, M. Elkashlan, and A. Nallanathan, "Joint altitude, beamwidth, location, and bandwidth optimization for UAV-enabled communications," *IEEE Commun. Lett.*, vol. 22, no. 8, pp. 1716–1719, Aug. 2018.

[18] W. Huang, Z. Yang, C. Pan, L. Pei, M. Chen, M. Shikh-Bahaei, M. Elkashlan, and A. Nallanathan, "Joint power, altitude, location and bandwidth optimization for UAV with underlaid D2D communications," *IEEE Wireless Commun. Lett.*, vol. 8, no. 2, pp. 524–527, Apr. 2019.

[19] J. Fan, M. Cui, G. Zhang, and Y. Chen, "Throughput improvement for multi-hop UAV relaying," *IEEE Access*, vol. 7, pp. 147732–147742, 2019.

[20] A. Fotouhi, H. Qiang, M. Ding, M. Hassan, L. G. Giordano, A. Garcia-Rodriguez, and J. Yuan, "Survey on UAV cellular communications: Practical aspects, standardization advancements, regulation, and security challenges," *IEEE Commun. Surveys Tuts.*, vol. 21, no. 4, pp. 3417–3442, 2019.

[21] A. Almohamad, M. O. Hasna, T. Khattab, and M. Haouari, "Maximizing dense network flow through wireless multihop backhauling using UAVs," in *Proc. Int. Conf. Inf. Commun. Technol. Converg. (ICTC)*, Oct. 2018, pp. 526–531.

[22] C. Qiu, Z. Wei, Z. Feng, and P. Zhang, "Joint resource allocation, placement and user association of multiple UAV-mounted base stations with in-band wireless backhaul," *IEEE Wireless Commun. Lett.*, vol. 8, no. 6, pp. 1575–1578, Dec. 2019.

[23] B. Perabathini, K. Tummuri, A. Agrawal, and V. S. Varma, "Efficient 3D placement of UAVs with QoS assurance in ad hoc wireless networks," in *Proc. 28th Int. Conf. Comput. Commun. Netw. (ICCCN)*, Valencia, Spain, Jul. 2019, pp. 1–6.

[24] Z. Zhu, L. Li, and W. Zhou, "QoS-aware 3D deployment of UAV base stations," in *Proc. 10th Int. Conf. Wireless Commun. Signal Process. (WCSP)*, Oct. 2018, pp. 1–6.

[25] X. Lin, V. Yajnanarayana, S. D. Muruganathan, S. Gao, H. Asplund, H.-L. Maattanen, M. Bergstrom, S. Euler, and Y.-P.-E. Wang, "The sky is not the limit: LTE for unmanned aerial vehicles," *IEEE Commun. Mag.*, vol. 56, no. 4, pp. 204–210, Apr. 2018.

[26] S. Boyd and L. Vandenberghe, *Convex Optimization*. Cambridge, U.K.: Cambridge Univ. Press, 2004.

[27] I. Polik and T. Terlaky, "Interior point methods for nonlinear optimization," in *Nonlinear Optimization*, G. Di Pillo and F. Schoen, Eds., 1st ed. New York, NY, USA: Springer, 2010, ch. 4.

[28] Z. Li, M. Chen, C. Pan, N. Huang, Z. Yang, and A. Nallanathan, "Joint trajectory and communication design for secure UAV networks," *IEEE Commun. Lett.*, vol. 23, no. 4, pp. 636–639, Apr. 2019.

YINGQIAN HUANG received the B.S. degree in communication engineering from Guangxi University for Nationalities, China, in 2017. She is currently pursuing the M.S. degree in information and communication engineering with the Guangdong University of Technology. Her current research interest is in unmanned aerial vehicle (UAV) communications.

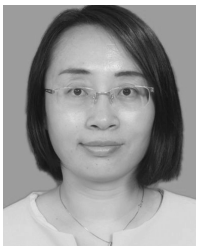

MIAO CUI received the B.E. degree in communication engineering and the M.S. degree in computer science from Northeast Electric Power University, Jilin, China, in 2001 and 2003, respectively, and the Ph.D. degree in circuit system from the South China University of Technology, Guangzhou, China, in 2009. She is currently a Lecturer with the Guangdong University of Technology, Guangzhou. Her research interests include the analysis, optimization, and design of wireless networks.

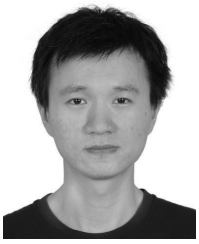

GUANGCHI ZHANG received the B.S. degree in electronic engineering from Nanjing University, Nanjing, China, in 2004, and the Ph.D. degree in communication engineering from Sun Yat-sen University, Guangzhou, China, in 2009. Since 2009, he has been with the School of Information Engineering, Guangdong University of Technology, Guangzhou, where he is currently a Professor. He was a Senior Research Associate with the City University of Hong Kong, from October 2011 to March 2012, and a Visiting Professor with the National University of Singapore, from January 2017 to January 2018. His research interests include MIMO and relay wireless communications, wireless power transfer, unmanned aerial vehicle (UAV) communications, intelligent reflecting surface (IRS), and physical layer security. He was a recipient of the IEEE Communications Society 2014 Heinrich Hertz Award and the IEEE Communication Letters 2014 Exemplary Reviewer.

WEI CHEN received the B.S. degree in resource exploration engineering, the M.S. degree in geotechnical engineering, and the Ph.D. degree in geological engineering from the Chengdu University of Technology, Chengdu, China, in 2002, 2006, and 2011, respectively. He worked with the Institute of Mountain Hazards and Environment, CAS, from July 2011 to December 2013. Since 2014, he has been with the Institute of Environmental Geology Exploration of Guangdong Province, Guangzhou, China, where he is currently a Senior Engineer. His research interests include geological disaster monitoring and forewarning.